Université Joseph-Fourier
CNRS-IN2P3

FR9003443

ISN 90.06
January 1990

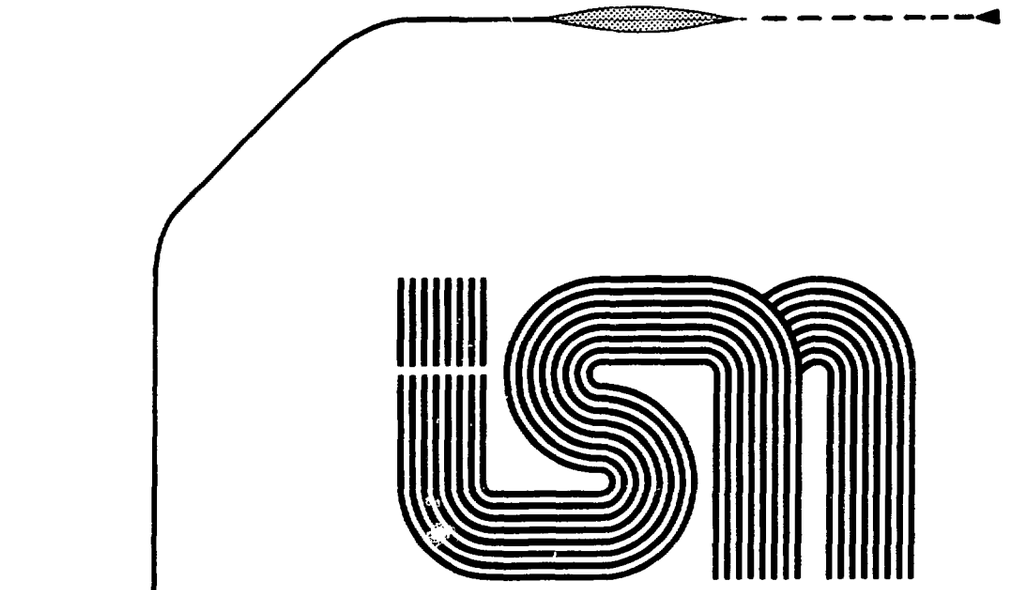

HIGH ENERGY PHOTONS PRODUCTION IN NUCLEAR REACTIONS

H.NIFENECKER* and J.A. PINSTON,

Institut des Sciences Nucléaires (IN2P3 , USTMG)
53, Avenue des Martyrs - F-38026, Grenoble Cedex, France

* and CEA/DRF/MDIH

Invited talk presented by H. Nifenecker at the "XXVIII Winter Meeting on Nuclear Physics, Bormio, January 22-26, 1990"

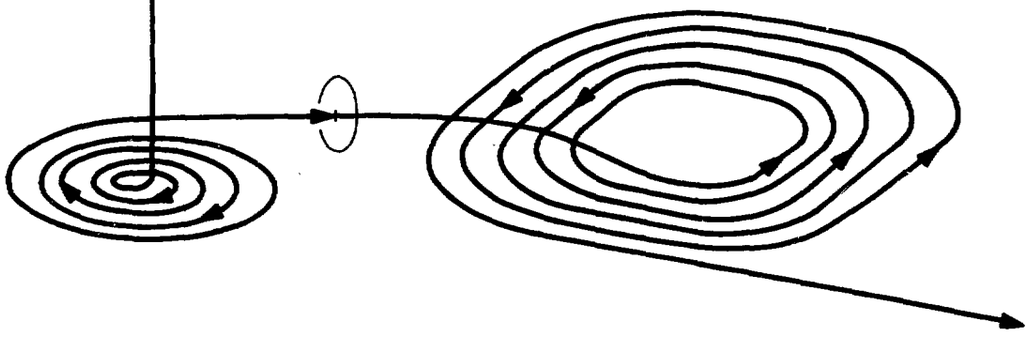

HIGH ENERGY PHOTONS PRODUCTION IN NUCLEAR REACTIONS

H.NIFENECKER* and J.A. PINSTON,

Institut des Sciences Nucléaires (IN2P3 , USTMG)
53, Avenue des Martyrs - F-38026, Grenoble Cedex, France

* and CEA/DRF/MDIH

INTRODUCTION

High energy gamma-ray production in heavy ion collisions has been the object of a number of recent studies between 15 and 120 MeV/Nucleon incident energies(1,2,3,4,5,6,7,8,9,10,11,12). Photons have attracted attention since they are not as seriously affected by absorption phenomena as pions, for example ; they can serve as unambiguous probes to study the reaction dynamics in the early stage of the collision. The main drawback of hard photon studies is the smallness of the γ-cross sections.

Several models have been proposed to predict the photon production yields. Some of them suggest that incoherent nucleon-nucleon bremsstrahlung is the main source of the γ-emission. These collisions can take place either in the initial stage of the reaction (13,14,15,16,17,18,19) or within an equilibrated hot participant zone (20,21). Other models suppose that photons are produced by coherent bremsstrahlung where both nuclei or substantial parts of them act as a whole (22,23,24). We shall see in Section 3 that the experimental results favor the first type of approach. In this approach where photons are produced as the results of an incoherent summation of the contributions of individual nucleon-nucleon-gamma processes, it is clear that a good knowledge of the cross-sections for these elementary reactions is needed.In the first section, we shall, therefore, review the experimental and theoretical aspects of these simpler reactions insofar as they relate to our main subject. It will appear that the contribution of charged pion exchange currents to photon production is very important. This is borne out both from new experimental results, which contradict some of the previous ones, and modern theoretical calculations.

The proton-Nucleus-gamma reactions provide an especially good and simple testing ground for models, and we shall give an account of both experimental results and theoretical calculations dealing with such processes, in section 2. Here again, recent experimental data contradict previous ones, and point to a large contribution of the charged pion exchange currents.

Dealing with the Nucleus-Nucleus reactions, our main emphasis will be with the inclusive measurements of differential production cross-sections. These include the shape of the spectra, the angular distributions and the absolute cross-sections. Results from exclusive reactions which display the impact parameter dependance of the multiplicity and spectra of the gamma-rays will also be presented, in section 3.1.

Finally, in section 3.2, we present an overview of the available theoretical approaches, and try to balance these different approaches with the experimental results, as well as with our knowledge of the more elementary processes.

1. NUCLEON-NUCLEON-GAMMA CROSS-SECTIONS.

Our experimental knowledge of the nucleon-nucleon-gamma production is irregular. The proton-proton system has been thoroughly studied (25,26), since it is the simplest, experimentally. In this case, a good measurement of the momenta and energies of the two protons, after scattering, is basically sufficient to describe the reaction. The neutron-neutron system is unknown, for obvious reasons. Our knowledge of the neutron-proton-gamma process is poor(27,28,29,30). This is due to the small intensity and bad resolution of the neutron beams. Furthermore the neutron and photon detectors are more difficult to build and less efficient than proton detectors. This is unfortunate since it is known, experimentally(31,32) and theoretically (20,33) that the n-p-γ process is, by far, more efficient than the p-p-γ process to produce gamma-rays.For this reason, we concentrate, in the following, on the n-p-γ reaction.

1.1 Experimental Data on the Neutron-Proton-Gamma Process.

Very few data have been reported on the neutron-proton-gamma process. Measurements were carried out at neutron beam energies of 130 MeV(34), 208 MeV(28), 72 MeV(29) and 180 MeV(30). Genuine n-p-γ measurements require neutron beams of high intensities and well defined energies. These neutrons are usually produced in p+Be or p+Li, as well as d+Be reactions.

In the first three cases, both scattered proton and neutron were detected in coincidence. In the non-relativistic limit, the momentum of the photon can be neglected. Then, any couple of scattering angles of the proton and neutron corresponds to a given gamma-energy. For moderately relativistic velocity of the incident particle, a narrow gamma-spectrum corresponds to each pair of scattering angles with respect to the beam. Detailed formula can be found in (11) for example. The n-p-γ differential cross-sections $\frac{d^2\sigma}{d\Omega_n d\Omega_p}$ for various neutron and proton exit angles, as obtained by Brady(34) and Edgington(32) were compiled by Remington(35) and Nakayama(36) and can be found in (11) . In general, the experimental results agree better with quantal calculations including charged mesons exchange currents contributions (33,36,37) than with semi-classical calculations (20,35).

The recent experiment of Pinston(30) used two gamma-ray telescopes where the shower energy were measured in large NaI scintillators positioned at 90° from the beam direction.The neutrons were obtained from a 400 MeV deuteron beam provided by the SATURNE facility stripped by transmission through a thickness of 12 cm of Berylium. The protons were magnetically swept out and the few remaining charged particles were discriminated against by an anticoincidence plastic scintillator, situated immediately downstream from a 8 meters stainless-steel collimator(38). Taking into account the average energy loss of the deuterons in the Berylium target, the average energy of the neutrons is found to be 175 MeV. The width of the spectrum was obtained from a time of flight measurement of the protons produced by charge exchange in a thin plastic scintillator. It was found to be approximately 80 MeV FWHM. A 20 cm long liquid Hydrogen target was used. A run, whith an empty target showed that the background was small.The beam intensity was monitored by a thin plastic scintillator and calibrated using the reaction $n + Al^{27} \Rightarrow Na^{24}$ using the assumption that this reaction had the same cross-section as the known $p + Al^{27} \Rightarrow Na^{24}$ reaction. A test of the calibration method was provided by the measurement of the photon spectrum produced in the n+C reaction, which, when measured at 90°, should be very close to that observed in the p+C reaction as measured at the Orsay Synchrocyclotron(39) with a proton energy of 168 MeV. Comparison between the P+C and n+C data is shown on Figure 1. The agreement is seen to be satisfactory. The spectrum observed in the n+H reaction, after background correction, at 90°, is shown on Figure 2, together with a theoretical calculation by Nakayama et al.(40).

It is also possible to extract information on the elementary n-p-γ process from the radiation emitted in p-d-γ reactions. Such studies are, also, scarce. Koehler and colleagues (31,41) measured

the p-p-γ and p-d-γ reactions at 148 MeV and 198 MeV. The comparison between the two reactions confirms that the p-p-γ contribution is small. The total cross-section measured at 148 MeV was 26 μbarns for gamma-energies larger than 25 MeV. Edgington and colleagues(32), measured p-d-γ reaction at 140 MeV. The integrated cross-section they found was 11 μbarns for the p-d-γ reaction and gamma energies larger than 25 MeV. This is, therefore, a factor of more than two less than the value found by the Rochester group(41).The results of Edgington(32) seem to favor calculations which do not incorporate internal contributions, while the reverse seems to be true for the Rochester results.

Pinston et al.(42) have carried out a measurement of the p-d-γ reaction at 200 MeV proton energy. The photon energy spectrum observed at several angles are shown on Figure 3, and compared with calculations of the elementary n-p-γ process. To our knowledge there exists no complete calculation of the p-d-γ reaction. However, it is clear that only calculations incorporating important internal contributions can account for the experimental data. This seems to point to some systematic error in the data of Edgington. That this is the case can also be seen from a comparison between their results on the p-Nucleus-γ process and those obtained by Pinston(39), as will be shown thereafter.

1.2 Theoretical Descriptions of the Neutron-Proton-Gamma Process.

The first nucleus-nucleus calculations have used the classical(14,15,20,35) approximation, with the inclusion of energy conservation, in the semi-classical fashion.The energy spectrum follows a $1/E_\gamma$ law, with a sharp cut-off at the maximum energy. In the non-relativistic approximation, the angular distribution characteristics are simply obtained (see section 3 of 11). Consider an elastic scattering process where Θ is the scattering angle. θ is the angle between the direction of the photon an that of the incident particle.In the non-relativistic approximation, the photon angular distribution reads(11):

$$\frac{dN(\theta)}{d\Omega} \approx \beta^2 \left(< sin^2\Theta > + sin^2\theta \left\{ 1 + < cos^2\Theta > - \frac{1}{2} < sin^2\Theta > \right\} \right). \quad (1.1)$$

For moderately relativistic velocities, the Doppler effect leads to an additional quadrupole term in 1.1.

QUANTUM CALCULATIONS The semi-classical treatment summarized above, suffers from many deficiencies. It does not incorporate the quantal nature of photons, except for the higher cut-off of the spectrum. A quantum perturbative treatment of the nucleon-nucleon gamma process was first given by Ashkin and Marshak(43), using a Yukawa nuclear potential which reproduced the n-p scattering data, as they were known at that time.They were able to obtain an analytic expression for the the photon production cross-section.The calculated cross-section goes to 0 when the gamma energy approaches its maximum value, in contrast to the semi-classical approximation.

The Ashkin-Marshak treatment does not give correct angular distribution since it does not include the Doppler shift of the gamma-rays. Their formalism has been modified by Kwato Njock(44) who has been able, again, to obtain an analytic formulation of the cross-section. This formalism has been used to calculate the proton-nucleus process(see Section 2).

For small gamma energies ($p \simeq p_0$) the spectrum goes like $\frac{1}{E_\gamma}$, while for high gamma energies ($p \simeq 0$) it goes like $\frac{\sqrt{E_\gamma^{max} - E_\gamma}}{E_\gamma}$.The gamma spectrum shape is not very sensitive to the detailed shape of the nuclear potential, as long as the photon wave length exceeds the nuclear potential range, or, equivalently, as long as the photon energy is less than the pion mass.

The Ashkin and Marshak approach considers only on-energy shell nuclear potential matrix

elements. This is a consequence of their assumption that $|p_i| \simeq |p_f|$. However, if the photon emission occurs before scattering, the energy of the proton may be significantly affected. Such off-energy shell effects were investigated by Brown(45) and Brown and Franklin(37). Neuhauser and Koonin(46) integrated the results of Brown and Franklin over the neutron and proton scattering angles, to obtain integral gamma-ray spectra. The same approach was used, again, by Nakayama(36).The inclusion of off-energy shell increases markedly the photon production close to the end of the spectrum. Neuhauser and Koonin suggest that this increase is due to the fast decrease of the nucleon-nucleon cross-section with incident energy. They account, partially for this effect by replacing the semi-classical cross-section at the center of mass incident energy E_0 , $\frac{d\sigma}{dE_\gamma}(E_0)$ by the geometrical mean $\sqrt{\frac{d\sigma}{dE_\gamma}(E_0)\frac{d\sigma}{dE_\gamma}(E_0 - E_\gamma)}$. In the preceeding, it was assumed that the nucleons suffered only one nuclear scattering. It is possible, however, that they might suffer several and that the photon might be emitted between two successive scattering. This corresponds to the so-called rescattering terms. The contribution of these terms is small(36,37).

In p-n scattering, charged pions may be exchanged.These transient pionic currents may lead to photon emission, with characteristics similar to that due to the rescattering process. However, here, the mass of the pion is small and, therefore, the bremsstrahlung emission is expected to be enhanced. Considering, as in the Ashkin-Marshak potential, a one pion exchange, the range of the potential is simply related to the pion mass by $\frac{1}{\lambda} = \frac{\hbar c}{m_\pi c^2} \simeq 1.4\ fermi$. As well known, this relation is obtained by use of the uncertainty principle which gives the off-energy characteristic time, and by the assumption that the pions propagate with the speed of light. Using the same assumptions, it is possible to obtain a rough estimate of the bremsstrahlung of the virtual pions. It is given, in comparison to the proton external contributions by:

$$\sigma_\pi^{rad} = \sigma_{pn}^{rad}\frac{1}{\beta^2}\int_0^\infty \left(1 - cos\frac{\omega x}{c}\right)e^{-\lambda x}dx \tag{1.3}$$

which gives:

$$\sigma_\pi^{rad} = \sigma_{pn}^{rad}\frac{1}{\beta^2}\frac{\left(\frac{E_\gamma}{m_\pi c^2}\right)^2}{1 + \left(\frac{E_\gamma}{m_\pi c^2}\right)^2} \tag{1.4}$$

We recall that, here, β is the velocity of the proton in the center-of-mass frame. As an example, for 150 MeV incident energy, the maximum enhancement factor is around 13, and around 7 at 300 MeV incident energy. It is, therefore, quite a significant effect.

Calculations incorporating explicitly the meson exchanges were made by Baïer and colleagues(33) in an OBE type calculation.They obtained rather satisfactory agreement with experiment. Brown and Franklin(37) used a non-local potential formalism which can be shown to incorporate pion exchange effects, via the finite range of the potential. As said, this analysis was used again by Neuhauser and Koonin(46) and by Nakayama(36). Nakayama, for example, divides the electromagnetic potential into three contributions: $V_{em} = V_{conv} + V_{magn} + V_{exch}$. In the calculation, the Nuclear interaction potential was the so-called Bonn potential(47). The dominant diagramms considered by Nakayama are displayed on Figure 4. The electric convective and the

magnetic terms make up the external contributions and are of dipolar character. The internal contributions include the rescattering and exchange terms and are at least of quadrupole character. Figure 5 shows some results obtained by Nakayama.The convective term shows the familiar E_γ^{-1} dependence at low energy, the infrared divergence.The exchange term, in the limit of small gamma energies, behaves like E_γ.

Although Nakayama uses a relativistic kinematic, his treatment of the electromagnetic interaction is not covariant. A fully relativistic treatment has been given by Shäffer et al.(48) who used the One Boson Exchange parametrization of the scattering amplitudes as given by Horowitz(49). The covariant treatment gives rise to pair terms, as displayed on Figure 4 where a virtual proton-antiproton pair is created. For pseudo-scalar couplings, it can be shown that these terms are the same as the so-called sea-gull contact contributions appearing in the non-relativistic limit, with pseudo-vector coupling. These terms appear to carry most of the exchange contribution. The difference between the results of the non-covariant(36) and covariant(48) calculations has been shown to be caused almost entirely(12) by the failure of Horowitz parametrization to account for the low energy resonant p-n scattering . This resonant behaviour enhances markedly the photon emission probability close to the kinematical threshold. The authors of (12) argue that this resonant behaviour should not be present in nuclear medium, due to the inhibiting effect of the Pauli blocking, in the intermediate scattering states.

2. HIGH ENERGY PHOTONS PRODUCTION IN PROTON-NUCLEUS REACTIONS.

Information on the p-n-γ elementary process can also be deduced from proton-nucleus reactions. In this case the phase space problem is much simpler to solve than for a heavy ion collision and thus, different theories of the p-n-γ elementary process can be tested.

2.1 Experimental Data on Proton-Nucleus-Gamma Reactions

are also very poor. In the early experiments of Cohen(50)and Wilson(51) the order of magnitude of the photon cross section have been measured. More complete data have been reported by Edgington and Rose at 140 MeV(32) . In this work the photon production cross sections were measured for a wide range of targets and angles.Several important results were obtained. The shapes of the spectra were similar for targets ranging between deuterium and lead. The scaling of the cross-sections followed a $\frac{N}{A^{1/3}}$ law. The angular distributions were forward peaked, and were similar for p-d-γ and p-C-γ or p-O-γ. All these characteristics led the authors to conclude that the origin of the photons were individual n-p collisions, as suggested, previously by Beckham(52).

Recently, new results have become available concerning gamma emission induced by 72,168 and 200 Mev protons colliding with several target nuclei(39,42,53).For all three energies,the $N_T A_T^{-1/3}$ scaling law was confirmed.The energy spectra for the p + Au at 72 MeV reaction are "harder" for forward than for backward production. This difference is an indication of a photon emission from a moving source. The source velocity is close to the nucleon-nucleon c.m. velocity. In this midrapidity frame the shape of the energy spectra measured at different angles are almost identical as observed in Figure 6.

Again, for the p + Tb reaction (39)at 168 MeV,the spectra are "harder" for forward than for backward production.The rapidity distributions, for the different targets measured, are nearly identical. The source velocity deduced from the centroid of the rapidity distribution, is close to the nucleon-nucleon c.m. velocity, $\beta = 0.28$, for photons below 85 MeV while it is substantially smaller than this value for photons above 85 MeV. This can be understood, in the frame of a nucleon-nucleon model of photon production, since high-energy gamma-ray requires a collision of the beam proton with a target neutron having a high velocity opposite to the beam. This tends to slow down the nucleon-nucleon center of mass, in the laboratory frame.

Table 1 shows the total cross sections for bremsstrahlung production with photon energies greater than 40 MeV and measured at 168 and 200 MeV respectively. At 168 MeV the contribution due to photons coming from the decay of the neutral pions is estimated to be less than 9% for C and 24% for Au respectively, of the total cross section for $E_\gamma > 40MeV$ while at 200 MeV bombarding energy the pion background represents a contribution of 46% for C and 59% for Au respectively, of the total cross section for $E_\gamma > 40MeV$. The cross sections displayed in Table 1 are corrected for the neutral pion contribution at 200 MeV.

The characteristics of the angular distributions suggest that the hard photons are mainly produced in p-n collisions. This mechanism was already suggested by Beckham(52) and Edgington(32). Under this assumption the γ production cross sections can be written as $\sigma_\gamma = \sigma_R P_n P_\gamma$, where σ_R is the total reaction cross section (54,55), P_γ is the probability to produce a photon in a single n-p collision and $P_n = \sigma_{np}N/(\sigma_{np}N + \sigma_{pp}Z)$ is the probability for the incident proton to collide with a target neutron. As expected from the first collision hypothesis the $P_\gamma$values deduced from these measurements and displayed in Table 1 are almost independent of the target and projectile combination.The 200 MeV data are less precise than the 168 MeV data due to the neutral pion subtraction. In Table 1 we have also given the p + d measurements of Koehler(31) at 197 MeV and Pinston(42) at 200 MeV. It is seen that the values of P_γ observed with deuterium are close to those observed with other nuclei.

NS.

In Figure 7 we have compared our data at 72 and 168 MeV with the previous measurements of Edgington and Rose(32) at 140 MeV . For this purpose the photon production cross-sections are displayed as a function of the reduced variable E_γ / E_{beam}. Using this variable we see that the curves corresponding to our 72 and 168 MeV measurements lie almost on top of one another, except for the highest energies. In contrast the curve corresponding to the measurement of Edgington and Rose lies very much below our data.

2.2 Theoretical Calculations of the Proton-Nucleus-Gamma

Following the approach first taken by Beckham(52), the photon production rates in proton-nucleus collisions are usually deduced from the elementary p-n-γ cross sections, under the assumption that the proton makes a collision with one of the target neutrons. The neutrons are affected by the Fermi motion and the Pauli exclusion principle is taken into account in the final state(14,15,18,53). The contribution to the radiation of the acceleration produced by the mean nuclear field has been estimated(14,52) and found to be small as compared to the nucleon-nucleon collisions. Two approaches have been used, in order to take into account the Fermi motion and Pauli Blocking. The most commonly used(12,14,15,53) consider particle-particle collisions between the incident proton and the target neutrons, characterized by their Fermi momentum distribution. The other approach(18) considers the incident proton as an exciton inside the target nucleus, and follows its decay via a Boltzmann Equation. In both cases gamma emission may occur when a nucleon-nucleon collision takes place. One defines, therefore, a probability for gamma emission per collision. This probability is not the free n-p-γ probability, due to Pauli blocking. Further, the incident energy of the proton is increased by an amount equal to the nuclear potential depth minus the Coulomb potential.

In the first theoretical attempts(12,14,15,18,53) the elementary cross-sections were assumed to be the semi-classical ones. These were, indeed in agreement with the p-d-γ measurement of Edgington and Rose(32) at 140 MeV. It appeared that, provided the p-d-γ cross-section was well reproduced, it was also possible to reproduce satisfactorily the p-Nucleus data, even in the frame of first collision models, like the Fermi gas(14,53). This points to an internal consistency of both the experimental results(32) and the calculations.

However, since we have seen that new measurements of the p-n-γ, p-d-γ and, more generally,

proton-nucleus-γ process seem to contradict the older measurements of Edgington and Rose, it is important to compare the new data to calculations similar to those just mentioned. Obviously, in order to regain agreement between the calculated results and the revised experimental data, one should modify the elementary cross-sections.

Kwato Njock has compared the p-nucleus-γ results at 72,168 and 200 MeV with a Fermi gas type calculation(44). Two different assumptions were made concerning the elementary n-p-γ cross-section. In the first, use was made of the model of Ashkin and Marshak(43), described in section 1. In this model, radiation from charged meson exchange is neglected.The calculation reproduces reasonably well the proton-Nucleus data of Edgington and Rose at 140 MeV(32).

In the second approach the formulation of Nakayama(36) was used. Here the contribution of the internal pionic current is explicitly accounted for and is shown to be several times larger than the pure external contribution. To keep calculation times reasonable, a simple interpolation scheme was used for the elementary cross-sections(11).The calculation which includes the internal OBpionic contributions(36) gives a much better agreement with experiment both at 72 and 168 MeV.

Nakayama(36,56) has, also, used his formalism for a comparison with the data of Edgington and Rose(32), concerning the p+Be reaction at 140 MeV as well as with the new data of Pinston et al. at 72 and 168 MeV(39,53). He makes use of the Fermi gas model of the nucleus, as has been described above. Nakayama considers the effective mass of the nucleons and the magnitude of nuclear potential as parameters. To obtain a reasonable fit to the data of Edgington and Rose(32), Nakayama found the unreasonable result that the Fermi momentum corresponded to normal nuclear matter density($1.36\ fm^{-1}$) while there was no nuclear mean field. Much more reasonable values were able to provide qualitative agreement with the new results of Pinston et al.(39). This can be seen on Figure 8 where the results of the calculation are compared with experiment. For the p+Tb reaction at 168 MeV, the calculation assumed an effective nucleon mass of 0.9m, with m the free nucleon mass, and a Fermi momentum of $1.04 fm^{-1}$which corresponds to approximately 45% of normal nuclear matter density, and a mean field potential energy of -42 MeV. The corresponding values for the p+Au reaction at 72 MeV are 0.9m and $k_F = 0.7\ fm^{-1}$. Note that larger values of the Fermi momentum would lead to larger cross-sections. In their calculation Nakayama and Bertsch use a parametrization of the exact elementary cross-section(36), which tends to inhibit the resonant effect mentioned above. This was not the case in the calculation by Kwato Njock. Note also that, at 168 MeV, the contribution of π_0 decays may be not negligible. It is estimated to account for at most 24% of the cross-section above 40 MeV.

Using a BUU calculation with a covariant determination of the elementary cross-section (48), Cassing et al.(12) have some difficulties reproducing the experimental data. Pion contributions may explain the discrepancy at 168 MeV proton energy. However, the discrepancy at 72 MeV proton energy seems to be genuine. Wether it may reflect a deficiency in the treatment of the elementary cross-section in medium is open to question. Indeed, if, as implied by the calculations of Nakayama, the photon producing interactions take place in a low density region, in medium effects may be less important, and the resonant effect may have to be considered seriously.

In conclusion, it appears that the internal charged pion exchange currents contribution is important, even dominant, in the n-p-γ process. The careful study of proton-nucleus, and, even more, of nucleus-nucleus reactions may, therefore, give the possibility to examine the in medium modifications of the pionic currents. The theoretical status is still not clarified in the p-Nucleus case, since it seems that different theory groups, although using, basically, the same elementary cross-sections, come to different conclusions. This appears to be especially true for the lowest energies.

3. HIGH-ENERGY PHOTONS PRODUCTION IN NUCLEUS-NUCLEUS COLLISIONS.

3.1 Experimental Results.

SPECTRAL SHAPES Above 20-30 MeV the gamma-ray spectra show a distinct exponential behaviour for all systems studied between 20 and 85AMeV incident energies (1,2,3,8,9,57,58). It is also found that the slopes of the spectra depend on the angle of observation,larger angles corresponding to steeper slopes. Figure 9 shows an example of such a behaviour. It suggests emission by a moving source.Figure 10 shows the systematics of the inverse slopes of the spectra as a function of the incident energy per nucleon, as measured at 90°, in order to suppress the Doppler effect. A close examination of the slope parameters observed by the same group, and at the same incident energy per nucleon, displays a systematic variation of the slopes with the mass of the target. In general more massive targets lead to larger values of the inverse slope parameter E_0 . Below 20 MeV, departures from the simple exponential behaviour are observed, which can be attributed to the presence of gamma-rays produced in the statistical decay of hot nuclei produced in the reaction.

The E_0 systematic reported on Figure 10 shows a smooth variation with the beam energy, $E_P$and one finds $E_0(MeV) \simeq \frac{1}{3}$to $\frac{1}{4}E_P(MeV/\mathrm{n})$. Cassing et al.(12) parametrize the variations of E_0 by:$E_0 = 1.1\left(\frac{E-V_c}{A_p}\right)^{0.72}$. Below 30 AMeV, the Bremsstrahlung and statistical components are difficult to separate experimentally and the E_0values reported in Figure 10 are somewhat uncertain. This is especially true for symmetric or almost symmetric systems(11).

ANGULAR DISTRIBUTIONS As an example the angular distribution analysis of the three $Kr + (C, Ag, Au)$ reactions at 44 MeV/n are reported in Figure 11. The data of the three systems studied are normalized to the Kr+Au reaction according to their relative γ-cross sections. The angular distribution is forward peaked ($\sigma(30°)/\sigma(153°) = 3.05$) and the shape is almost identical for the three targets used. The data are then consistent with a γ-emission from a recoiling source with a source velocity almost identical for the three reactions

Least-squares analysis of the experimental spectra, at different laboratory angles, allow the extraction of values of the source velocities. Figure 12 shows the results of such fits for a number of systems and show, once more, a clustering of the observed experimental values around the half beam velocity. However a slight tendancy seems to exist (8, 59), which biases the source velocity towards that of the nucleus-nucleus center of mass. This may be the effect of secondary collisions where the proportion of participants originating from the heavier nuclear partner is increased, as compared to the case of the primary ones. Angular distributions may be computed in the half-beam velocity frame. In this frame, the angular distribution is almost isotropic. However a small anisotropic component of E1 character is also apparent.The relative amplitude, α, of the E1 component increases with beam energy and takes the values α = 0., 0.25 (7) and 0.40 (2) respectively at 30, 44 and 60 MeV/n. At 84 MeV/n Grosse (2) has found a nearly isotropic angular distribution with a possible minimum at 90°.Such a behaviour is to be expected if the origin of the radiation is attributed to incoherent p-n or n-p collisions(11).However one should be aware that, as such, the characteristics of the angular distributions do not rule out a collective origin of the radiation, where each nucleus would radiate as an entity. In this case, also, the natural frame of reference, for not too high energy gamma rays, has half the beam velocity, at least for systems having the same charge densities(11).

The dependance of the angular distributions of the gamma-rays as function of the mass of the projectile and target has been systematically studied by the M.S.U. group (59). In particular, these authors have studied symmetric systems with different total masses. Figure 13 shows the angular distributions observed in the nucleon-nucleon center of mass frame. The energy of the

beams was 30 AMeV. For all cases a dipole component is apparent. Its intensity, relative to the isotropic component ranges between 0.29 and 0.49, in agreement with the values found in (8) and (2). In general, it seems that the intensity of the dipole component is a decreasing function of the total mass of the system. As pointed out by the authors(59), this might be a consequence of an increased influence of secondary collisions in the more massive systems.

SYSTEMATICS OF THE PHOTON PRODUCTION CROSS-SECTIONS The almost exponential shape of the spectra, above about 30 MeV gamma-energy allows a description of the production cross- section with only two constants, for example, the slope of the exponential and the value of the integrated cross-section above some specific energy. Due to the relevance of the nucleon-nucleon center of mass for the angular distributions, the knowledge of the cross-section at 90° lab. allows the estimation of the angle integrated cross-section within an error of around 20% . Compilations of a number of systems which have been studied so far can be found in (11) and (21).First nucleon-nucleon collisions, seem to be the main source of the high energy photons. In this hypothesis photons are produced when charged protons are accelerated or decelerated in the nucleon-nucleon interaction.Only neutron-proton (n-p) collisions are efficient to produce photons and proton-proton collisions can be neglected.(20, 31, 32)

In this first collision hypothesis the total γ-cross section in nucleus-nucleus collisions follows the simple relation :

$$\sigma_\gamma = \sigma_R \langle N_{np} \rangle P_\gamma \tag{3.1}$$

where $< N_{np} >$is the average number of first n-p collisions. An estimate of this number can be made from the equal participant model (11,20).

$$\langle N_{np} \rangle = \frac{\langle A_F \rangle}{A_P A_T} \left(Z_P N_T + Z_T N_P \right) \tag{3.2}$$

with $A_P, Z_P, N_P, A_T, Z_T, N_T$ the mass charge and neutron numbers of the projectile and target respectively. Here, it is assumed that $A_P \leq A_T$. $\langle A_F \rangle$ is the average mass of the participant zone.

$$\langle A_F \rangle = A_P \frac{5 A_T^{2/3} - A_P^{2/3}}{5 \left(A_T^{1/3} + A_P^{1/3} \right)^2} \tag{3.3}$$

$\sigma_R$is the total reaction cross section. Below 30 MeV photon energy a statistical component is present which cannot be subtracted experimentally. However it is possible to compare the differential cross sections, for the same value of the ratio (E_γ / E_O),where $E_O$is the inverse slope parameter. For this purpose, the quantity :

$$\frac{d^2\sigma(\theta = 90°)}{d\frac{E_\gamma}{E_0} d\Omega} \frac{1}{\langle N_{np} \rangle \sigma_R} \tag{3.4}$$

is plotted versus (E_γ / E_O) in Figure 14. for a number of examples. The product $\langle N_{np} \rangle \sigma_R$ is the scaling factor defined in Equation 3.1. Only small relative variations with beam energies are observed in Figure 14 for different nucleus-nucleus reactions, measured at beam energies between 30 and 85 AMeV .The quantity defined in Equation 3.4 is the differential probability to produce a photon in a single n-p collision, in the nuclear medium, at a fixed beam energy.

The equation of the universal curve obtained in Figure 14 writes :

$$\frac{d^2P_\gamma(\theta=90^\circ)}{d\frac{E_\gamma}{E_0}d\Omega} \simeq P_\gamma e^{-\frac{E_\gamma}{E_0}} \tag{3.5}$$

with $P_\gamma = 10^{-4}$/ sterad .This quantity is nearly constant in nucleus-nucleus collisions at beam energies between 20 and 85 MeV/n. Extraction of systematic trends as a function of the beam energy or projectile and target masses is difficult, due to residual experimental errors. To study such variations, it is more convenient to look for them within coherent sets of data obtained by the same group.

For a number of systems measured at energies at 85 AMeV, as well as for reactions induced by a Kr beam with 44 AMeV, P_γ seems to be only weakly dependent upon $< N_{np} >$(11). A slight decreasing trend as a function of the system mass seems to be present. There, also, seems to be a trend of the variations of P_γ with beam energy. One, first, observes(11) a decrease from a value close to 10^{-4} around 30 AMeV to 0.6 10^{-4} at about 45 AMeV, followed by an increase to approximately 10^{-4} at 85 AMeV. Apparently, a strong increase to 3.5 10^{-4} occurs when the incident energy reaches 124 AMeV(58). In any case, apart from this last energy, it is striking that formula 3.5 allows a prediction of the photon production cross-sections within 50% over a very broad range of projectile, target and beam energy combinations.

IMPACT PARAMETER FILTERED HIGH-ENERGY PHOTONS PRODUCTION

Only a few experimental results where the high-energy gamma-rays were observed in coincidence with specific reaction channels have been reported so far (57,60,61,62). In general, the gamma multiplicity follows the violence of the reaction, while the inverse slopes of the spectra are somewhat smaller for peripheral collisions than for central ones.(11,61,62).

A quantitative approach was taken by Kwato Njock et al.(57)and Herrmann et al.(60). Kwato Njock measured gamma ray spectra for different light particle mutiplicities in the $^{36}Ar+^{27}Al$ system at 85 AMeV. The gamma spectra had the usual exponential character in all cases. In line with the analysis presented in the inclusive case the gamma multiplicity for each particle multiplicity bin could be written:

$$M_\gamma(\nu, E_\gamma) = \frac{\sigma_\gamma(\nu)}{\sigma(\nu)} = \frac{P_\gamma}{E_0} N_{np}(\nu) e^{-\frac{E_\gamma}{E_0}} \tag{3.6}$$

The slope $E_o$was obtained from the γ spectra corresponding to the different bins. P_γ was taken from the inclusive measurement to be approximately10^{-4}.The numbers of n-p collisions for each bin $N_{np}(\nu)$ could thus be obtained. It was found that, indeed, the number of n-p collisions increases when the reaction becomes more violent.The number of n-p collisions was transformed into an average impact parameter , using the formalism of Nifenecker and Bondorf(20).Using this correspondance the variation of the slope parameter E_0 with the overlap of the projectile and target could be deduced and is shown on Figure 15. On the same figure have been added values obtained from inclusive measurements with various targets.It is, of course, tempting to explain the correlation observed in Figure 15. by the spatial dependance of the Fermi momentum distribution of the nucleons. The decrease of the nuclear density close to the nuclear surface would imply a softer momentum distribution, and therefore a softer photon spectrum.

Herrmann et al.(60) studied gamma production in the reaction $^{92}Mo+^{92}Mo$ at 19.5 AMeV. The gamma-rays were detected in coincidence with the two heavy nuclei resulting from the deep

inelastic scattering of the projectile and target nuclei. The gamma-ray multiplicity as well as the inverse slope of the spectra were found to increase with the total kinetic energy loss of both nuclei.In a first analysis, these characteristic were attributed to statistical emission by the heated fragments(60). However, Metag et al.(12,63) has carried out a more careful treatment, in which a good fit of the spectrum below 20 MeV was required from the statistical component which included the effect of quasi deuteron emission. Doing so they were able to disentangle the thermal and Bremsstrahlung components, as shown on Figure 16. It is possible to translate the kinetic energy losses into impact parameter, if one assumes a one to one correspondance between the two quantities. The variations of the multiplicity of photons of energies larger than 30 MeV with the so-deduced impact parameter is shown on Figure 17. On the same Figure we have reported the variations of the number of n-p collisions(20) with the impact parameter, after normalization to the multiplicity for the central impact parameter. The correlation between the multiplicity and the number of collisions is striking. This correlation shows that it is possible to use high energy photons multiplicity as a measure of the average impact paramemeter of specific reactions channels.

PHOTON EMISSION IN LIGHT NUCLEI COLLISIONS The characteristics of photons emitted in p-Nucleus reactions have many similarities with those oberved in Nucleus-Nucleus collisions (See Section 2 and reference 11). This is true for the angular distributions, the spectrum intensities and shapes. Some differences are observed, however. Departures from the exponential shape of the spectra are noticed close to the maximum energy and are, obviously, consequences of energy conservation. Similar effects can be observed on the angular distributions. The exponential parts of the spectra are less steep than those observed in Nucleus-Nucleus reactions with the same incident energy per Nucleon. This is a consequence of the absence of Fermi motion in the elementary projectile.

To some extent, it is true that the absence of Fermi motion and Pauli blocking in the proton projectile makes a detailed comparison between p-Nucleus-γ and Nucleus-Nucleus-γ processes rather uncertain. This is why the recent measurements of light ion-nucleus-γ processes by the MSU group,(65) are interesting.It is found that the relevant quantity is the beam energy per nucleon rather than the total energy of the beam. This agrees with first collision models, and not with thermal models. It also agrees with the trends observed with heavier projectiles.

3.2 Theories of Photon Emission in Nucleus-Nucleus Collisions.

It is possible to distinguish three main types of theoretical approaches to the hard photon production in Nucleus-Nucleus reactions. These approaches have also been applied to other types of problems, such as pion production or fast particles emission. We classify these models into collective, dynamical and thermal ones.

THE COLLECTIVE MODELS. In the extreme collective approach, the nuclei are considered as simple entities scattered in the field of one another(22.23).The predicted scaling law has a strong dependance upon the nuclear charges. For symmetric reactions, the collective model predicts a $\sigma_R Z^2 \sim Z^{8/3}$ dependence.Experiment points to a much slower $Z^{5/3}$ one, as shown by the validity of the scaling law described in section 2. For this reason, it seems that the extreme collective model does not apply to nucleus-nucleus collisions at intermediate energies.

In the extreme collective model the collectivity is a property of the nuclei which behave like entities, all nucleons feeling simultaneously the accelerating fields, due to a very low compressibility. If one considers, at the opposite, that the nuclei are mere collections of nucleons interacting independently with one another, the electromagnetic field, itself, is a possible source of collectivity, due to its additive properties.The expected collectivity is small(20) since positive interferences

between collisions involving protons from the same nucleus tend to be cancelled by negative interferences with collisions involving neutrons from this nucleus.The emitted radiation is the result of fluctuations in the individual scattering processes, especially in the distribution of final parallel velocities, after scattering of two nucleons(11). The collectivity of the radiation, if it exists, decreases with gamma-energy.A quantum calculation(65) based on the quantum molecular model for nucleus-nucleus collisions obtains a residual collective component for the lowest photon energies, namely, below 30 Mev. Such results justify the treatment of photon production in nucleus-nucleus reaction as an incoherent summation of individual n-p-γ processes.

DYNAMICAL CALCULATIONS , with a few exceptions(65), have used this assumption extensively. In such calculations, the evolution of the phase-space distribution of the nucleons is followed in time, while individual nucleon-nucleon collisions eventually produce photons. Different approaches correspond to different simplification schemes of the phase space problem. In the mostcomplete approach the phase space distribution evolution is derived from an extension of the Boltzmann equation to Fermionic ensembles. There are several denominations for, basically, the same equation which has been used to follow the evolution of the phase space distributions. In the following, we shall retain the single denomination

Boltzmann-Uehling-Uhlenbeck(BUU), since it has been the most used in the frame of photon production calculations.This analysis has been extensively applied by the MSU,Giessen collaboration using either, the semi-classical n-p-γ cross-section (13,15) or a relativistic σ,ω model (66). One of the striking results of these calculations is the time evolution of the gamma emission.As a consequence of the Liouville theorem, a hole develops, in phase space, in the region of small relative velocities, enhancing photon production. Subsequently, due to the two-body collisions, the hole fills up. This filling up prevents further photon emission. It is found, that, for the C+C reaction at 84 AMeV, virtually all photons are emitted in a time smaller than $1.510^{-22} sec$. A close correlation between the photon yield and the number of first proton-neutron collisions is found.At low incident projectile energies, a broad range of experimental results was satisfactorily reproduced. However, it appeared that the calculation, above 50 AMeV projectile incident energy, seriously underestimated the experimental results. The inclusion of charged pion exchange contributions to the elementary cross-sections(48) alleviates this discrepancy quite significantly. This improvement is illustrated on Figure 18, taken from(12). The calculated photon yields follow, approximately, a $A_p^{0.91} A_T^{0.91}$ law, close to the observed one. The angular distributions are reasonably well reproduced. Similarly, the impact parameter dependence of the spectra is well reproduced, as can be seen on Figure 17.

Results very similar to those just described have been obtained with two other simpler approaches, the preequilibrium model of Remington and Blann(18), and the exchange model of Randrup and Vandenbosch(19).

It might seem surprising that three models as different as the BUU, BME and nucleon exchange give comparable results, concerning the high energy photon production. In fact, except, possibly, for the BUU calculations,it is a common feature of these models to have, first, been devised in order to take into account the fast particle preequilibrium emission. This was used to normalize the elementary nucleon-nucleon scattering cross-sections, both in the preequilibrium(BME) and in the nucleon exchange models.This defined the number of nucleon-nucleon collisions, and, therefore,the photon production cross-section, from the photon production rate per collision.

Although the dynamical calculations show that hard photons are produced dominantly in the first collisions, a significant fraction of them can still be produced in secondary collisions. Of course, after some kind of equilibration has occured, photons are produced thermally. If the life-time of the thermal source is long enough, its contribution could dominate the first collision one. This possibility might justify the

THE THERMAL MODELS approaches(1,20,67,68,69) .These models usually overestimate the hard photon production rate by almost an order of magnitude. In general they predict a faster increase of the photon production with the size of the system than actually observed. They are not able to reproduce the source velocity systematics without making ad hoc assumptions.

They have, also, great difficulties in explaining two important experimental features:
a) the similarities of the p-nucleus and nucleus-nucleus reactions. It is difficult to imagine an equilibrated hot zone made of only two or three nucleons.
b) the existence of an anisotropic component in the angular distribution. Resorting to angular momentum effects would not be helpful, here, since the anisotropy appears to be larger for small systems(64).

However, the breakdown of the thermal model approach to high energy photon production carries interesting information on the dynamics of the nucleus-nucleus reaction. In fact, if any object like a very hot participant nucleus existed, in an equilibrated state, for a finite amount of time, a thermal component should be present, in the photon spectra. The absence of this component tells us that the participant zone has a very short life-time, governed by dynamical instabilities.

SUMMARY AND OUTLOOK.

Hard photon production, in nucleus-nucleus collisions, has been studied at beam energies between 10 and 125 AMeV. From these measurements, the main characteristics of the photon emission have been deduced.It is found that the photons are emitted in a frame having close to the half beam velocity, that is the velocity of the nucleon-nucleon center of mass. In this frame, the angular distributions are symmetrical with respect to 90°with, in most cases, a dipolar character built upon an isotropic component. The spectra have almost exponentially decaying shapes, above 20 MeV, the inverse slope of which increase almost linearly with beam energy per nucleon. These characteristics are found for very light systems, like d+C or Li−Li as well a for very heavy ones like Kr+Au or Xe+Sn. The photon production yields follow a very simple scaling rule, which relates them to the number of first n-p collisions.

These characteristics of the photon emission suggest strongly that the neutron-proton collisions in the early stage of the reaction are the main source of high energy γ-rays.

Some hints of a second stage of knowledge are already present in recent data. The slopes of the spectra, for the same beam energy per nucleon, seem to depend .in a significant way, upon the target mass, as well as upon the impact parameter. This may be a consequence of changes in the Fermi motion of nucleons, from system to system.

The angular distributions appear to be more anisotropic for lighter systems than for heavier ones. This may be a signal of a persisting influence of multiple collisions, which becomes more important in heavy systems.

Although the scaling law gives a photon emission probability per n-p collision which appear remarkably, and surprisingly, constant for the large variety of systems studied so far, some significant variations are probably present. It is, still difficult to extract them, due to the different experimental and analysis techniques used by the different groups.There is, however, some evidence that this emission probability increases with beam energy.

The only theoretical approaches which have been, so far, able to reproduce the main trends of the data are dynamical calculations which evaluate the number of nucleon-nucleon collisions as a function of time. To each such collision is associated a small but finite probability for photon emission. These calculations show that, indeed, most photons are produced early in the collision. They, also, associate closely photon and fast particle emission. However, these calculations, when using semi-classical expressions of the elementary nuceon-nucleon-γ cross-section, are not able to repro-

duce the shape of the photon spectra, above, approximately, 60 AMeV incident energy. This failure is due to the important contribution of charged pion exchange currents to the photon production. This importance is demonstrated in recent p-nucleus-γ and n-p-γ experimental studies. Theoretical attempts to include these contributions in calculations of p-nucleus-γ and nucleus-nucleus-γ reactions show significant improvements in their account of the experimental data.

Future experimental work should aim at reducing the remaining systematic errors, so that a precise study of the effects of multiple collisions could be carried out. Exclusive experiments will certainly be realized, in order to investigate the change of spectral shapes, as well as angular distributions, with impact parameter. These studies may lead to the observation of unambiguous collective effects, which we have failed to identify, so far, although they have been predicted. The impact parameter dependence of the photon yields may, also, be used as a tool in studying heavy-ion reaction mechanisms. At the higher energy range the contribution to the gamma spectra of the neutral pions decays has to be precisely estimated, so that we could gain knowledge of photon production at energies as high as possible. At those energies, it is expected that Fermi and Pauli effects would be minimized, leading, therefore, to an easier analysis of the production mechanisms.

The most needed experimental work is a careful and extensive study of the elementary n-p-γ process. The study of small systems, like p-d, d-d , α-p is also important.

One of the most exciting perspective offered by the study of hard photon emission in nucleus-nucleus reactions is the possibility to examine,if and how much the nuclear medium modifies the elementary n-p-γ process. Such modifications are expected, for example, if the pion mass, in nuclear matter, is different from its vacuum value. In this context, it is important to note that it seems that, above 50 MeV, most photons are produced by the exchange currents. Photon production is, probably, the most sensitive probe of charged pions exchange currents.

ACKNOWLEDGEMENTS. It is a pleasant duty to thank N.Alamanos, W.Bauer, W.Benenson, G.Bertsch, J.P.Bondorf, W.Cassing, M.Durand, A.Gobbi, E.Grosse, C.Guet, K.Knoll, M.Blann, V.Metag, U.Mosel, M.Prakash, J.Randrup, B.Remington, J.Stachel, J.Stevenson, R.Vandenbosch for many illuminating discussions and for providing us with unpublished data.The part of the work reported here in which we had a personal contribution was done with the invaluable help of D.Barneoud, V.Bellini, S.Drissi, B.Guillot, J.Julien, J.Kern, M.Kwato Njock, M.Maurel, C.Ristori, F.Schussler., J.P.Vorlet, Y.Shutz

We thank deeply the staffs of the following accelerators: GANIL, Orsay SC, SARA, SATURNE, SIN cyclotron where our experiments were carried through.

We aknowledge the support of the Institut des Sciences Nucléaires and of the Département de Recherche Fondamentale, Grenoble, where most of this work was carried on. More especially we thank B.Vignon for the constant interest he has shown in our work.

REFERENCES.

1.Grosse,E., In H.Feldmaier(Ed.), *Proc. Intern. Workshop on Gross Properties of nuclei and nuclear excitation, Hirshegg*,65(1985).
2.Grosse,E. et al., *Europhys. Lett.2*: 9(1986)
3.Stevenson,J. et al., *Phys.Rev.Lett,57*: 555(1986).
4.Stevenson,J. et al., *Nucl. Phys.A471*:371c(1987).
5.Alamanos,N. et al., *Phys.Lett.173B* :392(1986).
6.hingmann,R., *Thesis*(1987).
7.Bertholet,R.et al., *Journal de Physique.C4*:201(1986).
8.Bertholet,R.et al., *Nucl.Phys.A474*:541(1987).
9.Kwato Njock,M. et al., *Phys. Lett.B175*:125(1986).
10.Clayton J. et al., *Phys.Rev.C40*:1207(1989)
11.Nifenecker,H. and J.A.Pinston., *Prog. in Part. and Nucl. Phys.* 23:271(1989)
12.Cassing,W. et al. to be published in *Physics Reports*(1989).
13.Cassing,W. et al., *Phys.Lett.181B*:217(1986).
14.Nakayama,K. et al., *Phys. Rev.C34*:2190(1986).
15.Bauer,W. et al., *Phys.Rev.C34*:2127(1986).
16.Bauer,W. et al., *Proceedings of the XXV Intern. Winter Meeting on Nuclear Physics, Bormio, Italy, Jan.(1987).*
17.Che Ming Ko and J.Aichelin, *Phys. Rev.C35*:1976(1987).
18.Remington,B.A. et al., *Phys.Rev.Lett.57*:2909(1987).
and *Phys. Rev.C35*:1720(1987).
19.Randrup,J. and R.Vandenbosch,*Nucl.Phys.A490*:418(1988)
20.Nifenecker,H. and J.P.Bondorf, *Nucl.Phys.A442*:478(1985).
21.Prakash,M.et al., *Phys.Rev.C37:1959*(1988).
22.Vasak,D. et al., *Journ. of Phys.G11*:1309(1985).
23.Vasak,D., *Phys. Lett.176B*:276(1986).
24.Stahl,T. et al., *Zeit. für Phys.A327*:311(1987).
25.Signell,P., Some theoretical Aspects of p-p Brehmsstrahlung.in G.Paic and I.Slaus(Ed.),*Few Body problems,light Nuclei and Nuclear Interactions.* Vol.1:287(1967).
26.Kitching,P. et al., *Nucl. Phys.*A463:87c(1987).
27.Brady,F.P. and J.C.Young., *Phys. Rev.C2*:1579(1970).
28.Edgington,J.A. et al., *Nucl. Phys.A218*:151(1974).
29.Dupont,C. et al., *Nucl.Phys.A481*:424(1988).
30.Pinston,J.A., S.Drissi, J.Julien, F.Malek, H.Nifenecker and F.Schussler unpublished (1989).
31.Koehler,P.F.M.et al., *Phys.Rev.Lett.18*:933(1967).
32.Edgington,J.A. and B.Rose., *Nucl. Phys.89*:523(1966).
33.Baïer,R. et al., *Nucl.Phys.B11*:675(1969).
34.Brady,F.P., et al., *Phys.Rev.Lett.20*:750(1968).
35.Remington,B.A. and M.Blann, *Phys.Rev.C36*:1387(1987).
36.Nakayama,K., *Phys.Rev.C39*:1475(1989)
37.Brown,V.R. and J.Franklin. *Phys. Rev.C8*:1706(1973).
38.Bizard G. et al., *N.I.M.111*:451(1973)
39.Pinston,J.A. et al., *Phys.Lett.B218*:128(1989)
40.Herrmann,V., J.Speth and K.Nakayama, to be published(1989)
41.Rothe,K.W. et al., *Contribution to the Williamsburg Conf. on intermediate energy physics*,(1966)
42.Pinston,J.A., D.Barnéoud, V.Bellini, S.Drissi, J.Guillot, J.Julien, H.Nifenecker and F.Schussler unpublished (1989)

43.Ashkin,J. and R.E.Marshak, *Phys.Rev.76*:58(1949).
44.Kwato Njock,M., *Thesis*. Univ. Joseph Fourier. Grenoble(1988).
45.Brown,V.R., *Phys.Rev.170*:1498(1969).
46.Neuhauser,D. and S.E.Koonin, *Nucl. Phys.A462*:163(1987).
47.Messiah.A, *Mécanique Quantique*, Dunod(1959)
48.Schäfer,M. et al., *Phys.Lett.221B*:1(1989)
49.Horowitz,C.F., *Phys.Rev.C31*:1340(1985)
Murdock,D.P. and C.F.Horowitz, *Phys.Rev.C35*:1442(1987)
50.Cohen,D. et al., *Phys. Rev.130*:1505(1963).
51.Wilson,R., *Phys. Rev.85*:563(1952).
52.Beckham,C., *Thesis* University of Berkeley(1962).
53.Kwato Njock,M. et al., *Phys. Lett.B207*:269(1988).
54.Bauhoff,W., *Atomic and Nucl. Data Tables 35*:429(1986).
55.Hess,W.N, *Rev. of Mod. Phys.30*:368(1958).
56.Nakayama,K. and G.F.Bertsch, Phys.Rev.C40:685(1989)
57.Kwato Njock,M.et al., *Nucl.Phys.A488*:503c (1988)
58.Clayton J. et al., *Phys.Rev.C40*:1207(1989)
59.Tam,C.L., et al., *Phys.Rev.C39*:1371(1989)
60.Herrmann et al., *Phys.Rev.Lett.60*:1630(1988).
61.Hingmann,R. et al., *Phys.Rev.Lett.58*:759(1987).
62.Gaardhoje,J.J et al., *Phys. Rev.Lett.56*:1783(1987).
63.Metag,V, A.Gobbi, K.Hagel, N.Herrmann and W.Kühn,
to be published(1989)
64.Tam,C.L., et al., *Phys.Rev.C38*:2526(1989)
65.Heuer,R. et al., *Z. für Phys. Atomic Nuclei 330*:315(1988).
66.Biro,T.S. et al., *Nucl. Phys.A475*:579(1987).
67.Shyam.R. and J.Knoll. *Nucl.Phys.A448*:322(1986).
68.Prakash,M. et al., *Phys.Rev.C33*:937(1986).
69.Bonasera,A. et al., *Nucl.Phys.A483*:738(1988).

FIGURE CAPTIONS.

Figure 1 Comparison of the photon spectra observed in the $p+^{12}C$ and $n+^{12}C$ reactions at 168 MeV and 180 MeV beam energies respectively. Due to the difference of beam energies, the photon energies are plotted on a reduced scale E_γ/E_{beam}. For the same beam energy, isospin symmetry considerations lead to the expectation that the two spectra should be almost superimposed. The experimental situation agrees with that prediction.

Figure 2 Comparison of the photon spectrum observed at 90°, in the reaction n+p at 180 MeV neutron energy with a theoretical calculation (40). Here, use was made of the parametrized form of the n-p-γ cross-section, as given in reference 40.

Figure 3 Photon spectra observed at three laboratory angles in the reaction p-d-γ at 200 MeV proton energy. Also shown on the figure (continuous lines) are the results of a theoretical calculation for the n-p-γ reaction at 200 MeV, in the absence of a reliable calculation of the p-d-γ process.

Figure 4 Most important diagramms contributing to photon production in the n-p-γ process.

Figure 5 Various contributions to the photon production (36) for neutron-proton reactions at 150 and 300 MeV, at θ=30°.– · – · Magnetic contribution.– – – Convection contribution.· · · Exchange contribution._ _ _ Total cross-section.

Figure 6 Energy spectra of high energy photons for the p+Au reaction at 72 MeV, measured at $\theta_{lab} = 30°, 90° and 150°$.and transformed in the nucleon-nucleon c.m. frame.

Figure 7 Comparison, in a reduced plot, of our results at 72 (squares)and 168 MeV (triangles) with those of Edgington and Rose(32) at 140 MeV(crosses). The system studied was p + Au at 90°.

Figure 8 Bremsstrahlung differential cross section(in the laboratory system) for $p+^{159}Tb$ at 168 MeV proton energy, as a function of photon energy and for different photon emission angles. The value of the Fermi momentum and effective masses used in the calculation were $k_F = 1.04\ fm^{-1} and m^* = 0.9m$, respectively. The calculations are from reference 56 and the data from reference 39.

Figure 9 Photon energy spectra, at different laboratory angles, for the reaction $^{86}Kr +^{197} Au$ at 44 AMeV.

Figure 10 Inverse slope E_0 versus beam energy.The bars correspond to E_0 variations for different projectile-target combinations.

Figure 11 Plot of the laboratory angular distribution of high energy photons for the $^{86}Kr -^{197} Au$ reaction at 44 MeV/n.The angular distribution for $Kr + C$ and $Kr + Ag$ reactions are also reported on the same plot; they are normalized to the$^{86}Kr +^{197} Au$ reaction according to their total γ-cross sections . The solid line is the result of a BUU(12) calculation for $^{86}Kr +^{12} C$.

Figure 12 Variations of the source velocity with the incident energy of the beam.

Figure 13 Angular distributions as observed in the half velocity frame.(59)

Figure 14 Plot of the invariant quantity $\frac{d\sigma(\theta=90^\circ)}{dx}\frac{1}{\sigma_R<N_{np}>}$ as a function of $x = \frac{E}{E_0}$ for different systems.

Figure 15 Variation of the inverse slope E_0 with the overlap distance between projectile and target $R_P + R_T - b$. The impact parameter b was obtained from the number of participants $< A_F >$, using the formalism of Nifenecker(20).

Figure 16 Multiplicity of high energy photons(E_γ>30 MeV) decomposed into a thermal and a bremsstrahlung contribution, respectively. the multiplicities are plotted as a function of the total kinetic energy loss for the system $^{92}Mo + ^{92}Mo$ at 19.5 AMeV. (From Reference 12)

Figure 17 Impact parameter dependence of the photon multiplicity for the system $^{92}Mo + ^{92}Mo$ at 19.5 MeV. The continuous curve is the result of a BUU calculation(12), the dashed curve is obtained from the equal participant model(20).

Figure 18 Photon energy spectra from heavy-ion collisions. The solid lines are the result of a BUU calculation based on the scalar meson exchange(66) and the dashed lines are the results of the BUU calculation using the effective meson exchange approximation(48). The experimental data come from references 2 and 3. The emission angle is 90° in all cases.
○ 84 AMeV $^{12}C + ^{12}C$; 40 AMeV $^{14}N + ^{12}C$; 30 AMeV $^{14}N + ^{12}C$; ◇ 20 AMeV $^{14}N + ^{12}C$

Table 1 - Photon cross sections and P_γ values at 168 and 205 MeV for $E_\gamma > 40MeV$. The $p + d$ cross sections comes from (31) and (39).

$TARGET$	$E_p = 168MeV$	$E_p = 168MeV$	$E_p = 200MeV$	$E_p = 200MeV$
	$\sigma_\gamma(\mu b)$	$P_\gamma x 10^4$	$\sigma_\gamma(\mu b)$	$P_\gamma x 10^4$
C	90 ± 9	5.7 ± 0.6	155 ± 32	9.8 ± 2.0
Al	221 ± 22	6.4 ± 0.6		
Cu	361 ± 36	6.1 ± 0.6		
Ag	606 ± 61	7.0 ± 0.7	1049 ± 208	12.1 ± 2.4
Tb	806 ± 81	6.1 ± 0.6		
Au	911 ± 91	6.3 ± 0.6	910 ± 269	6.3 ± 1.9
$d(31)$			23 ± 4	5.1 ± 0.8
$d(39)$			37 ± 3	8.2 ± 0.8

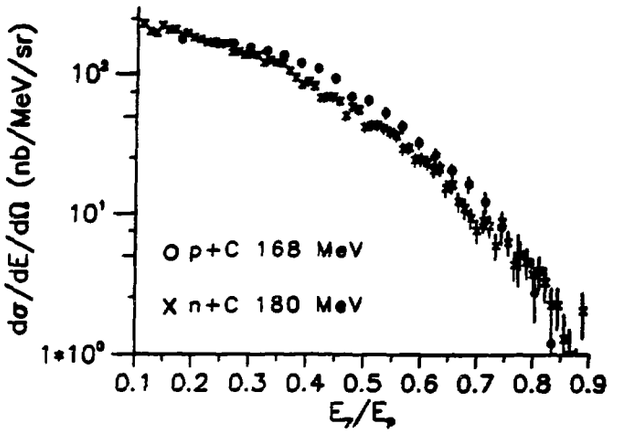

FIGURE 1

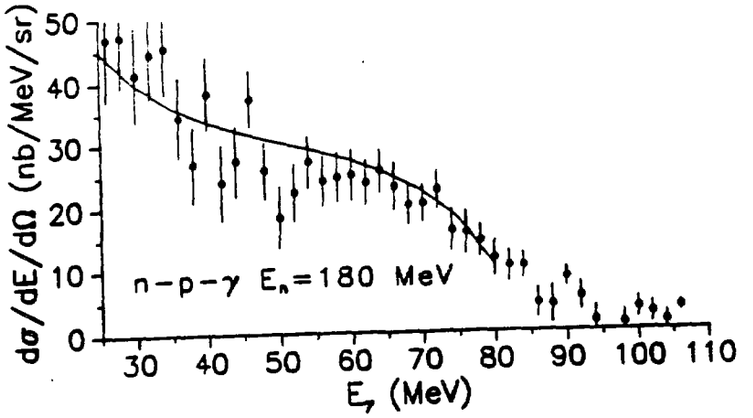

FIGURE 2

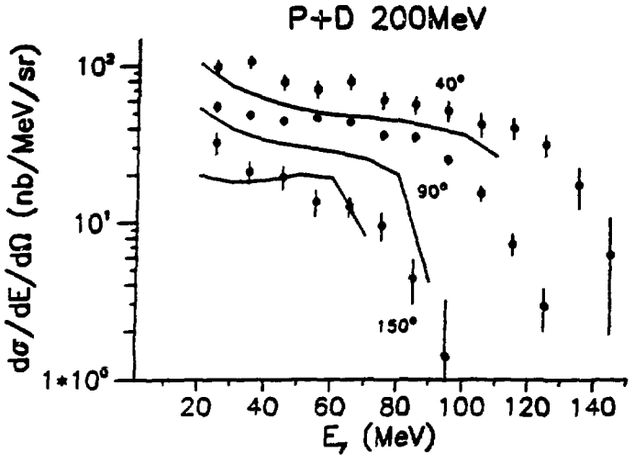

FIGURE 3

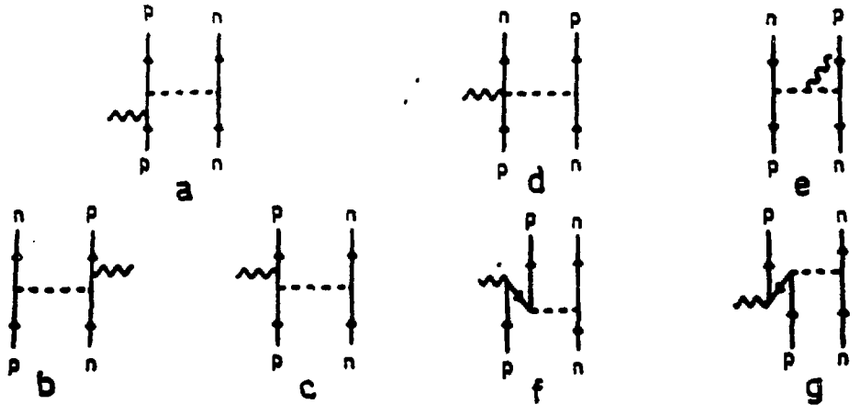

FIGURE 4

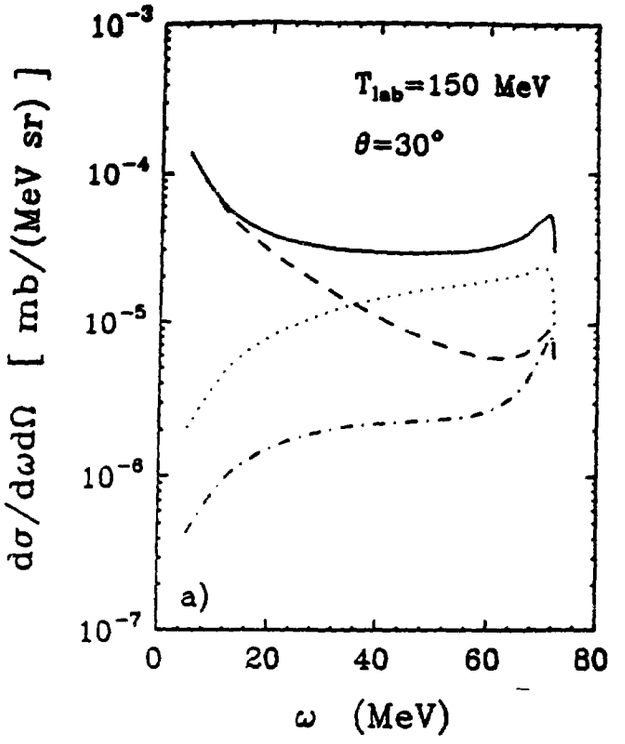

FIGURE 5

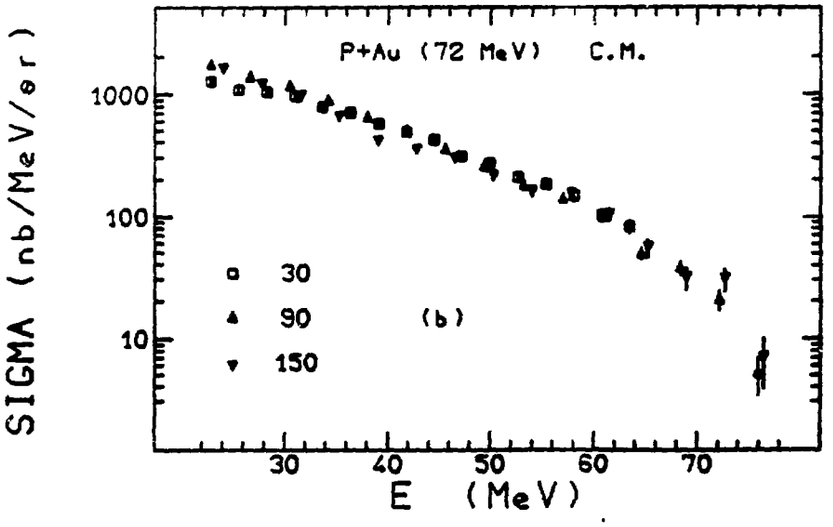

FIGURE 6

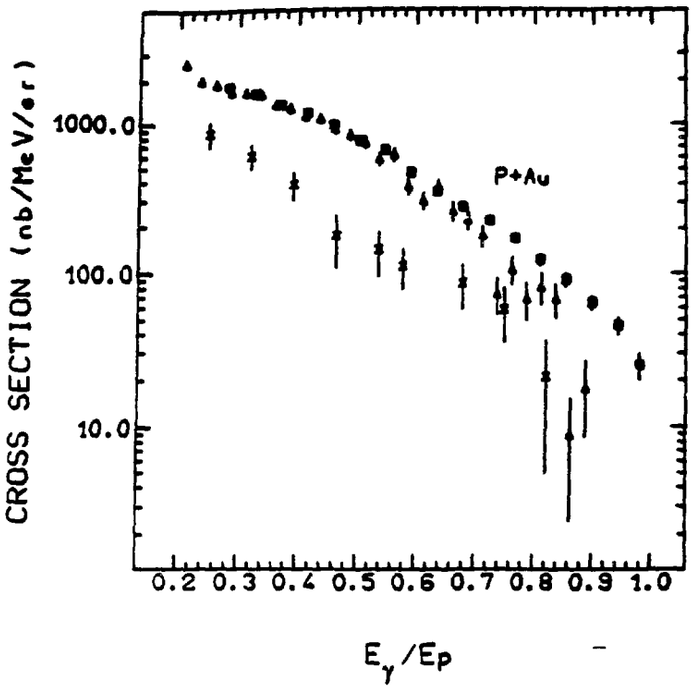

FIGURE 7

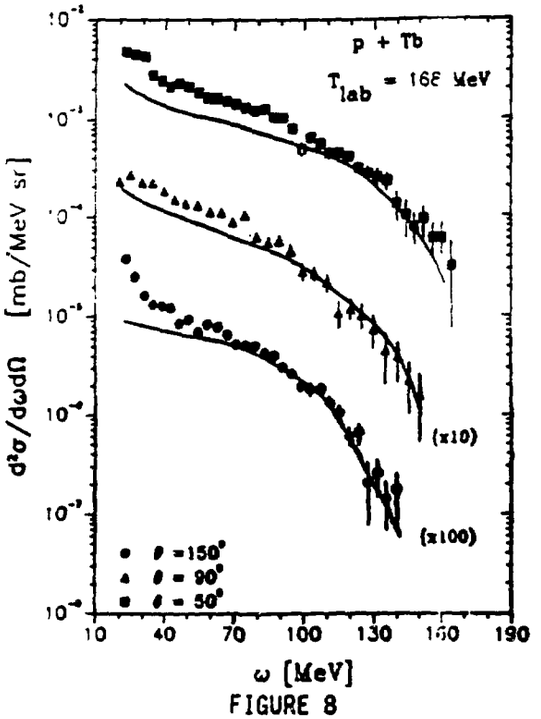

FIGURE 8

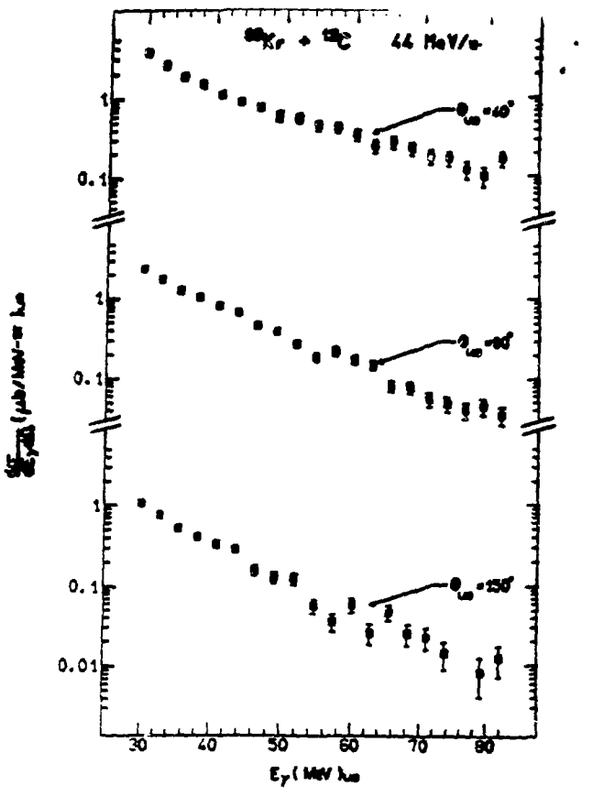

FIGURE 9

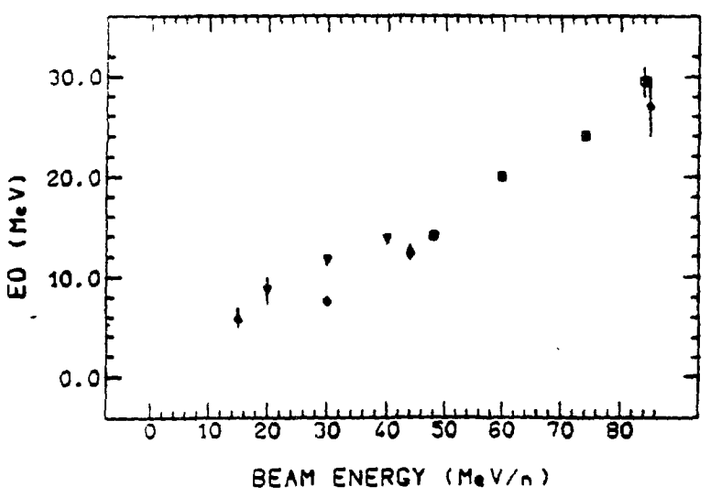

FIGURE 10

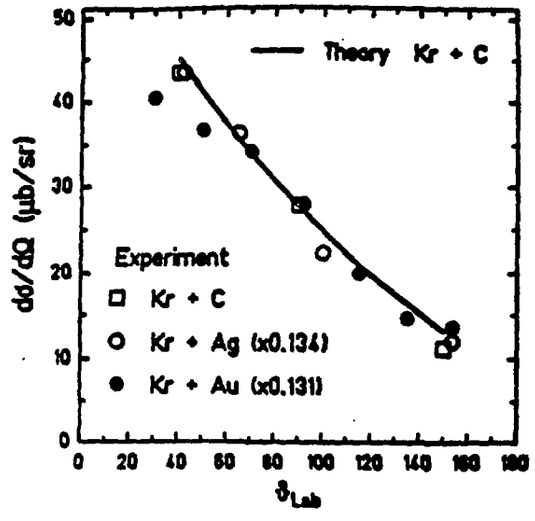

FIGURE 11

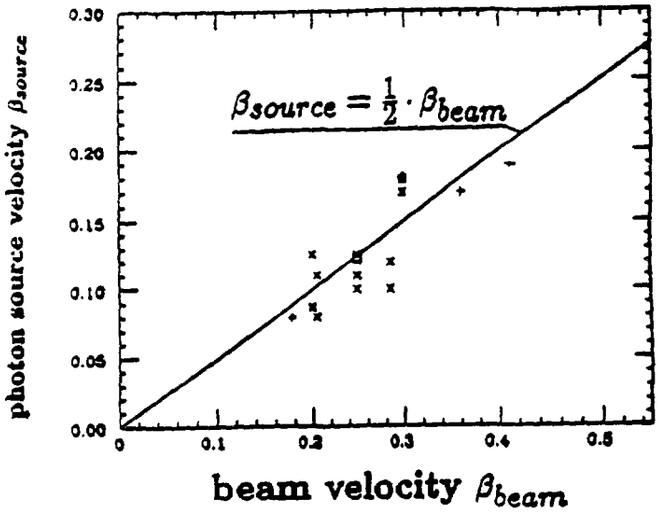

FIGURE 12

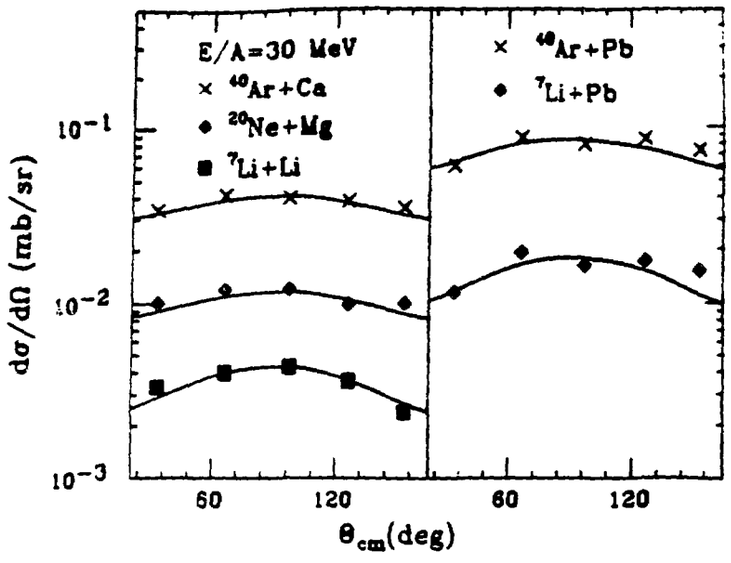

FIGURE 13

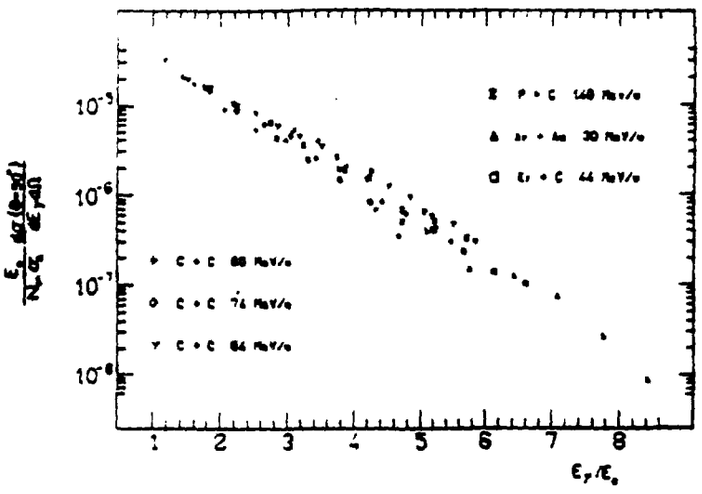

FIGURE 14

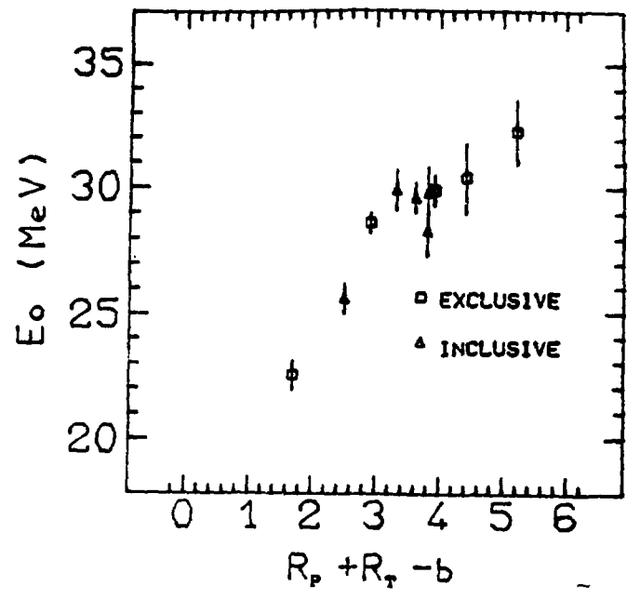

FIGURE 15

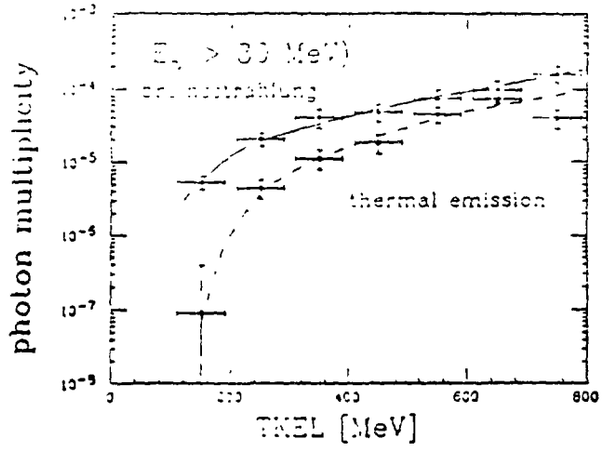

FIGURE 16

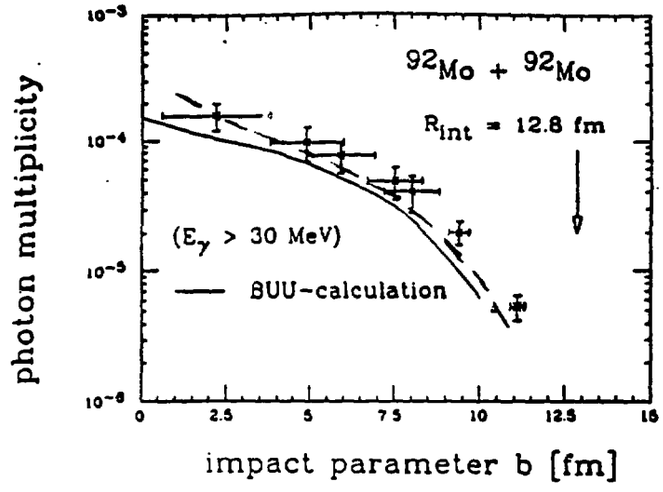

FIGURE 17

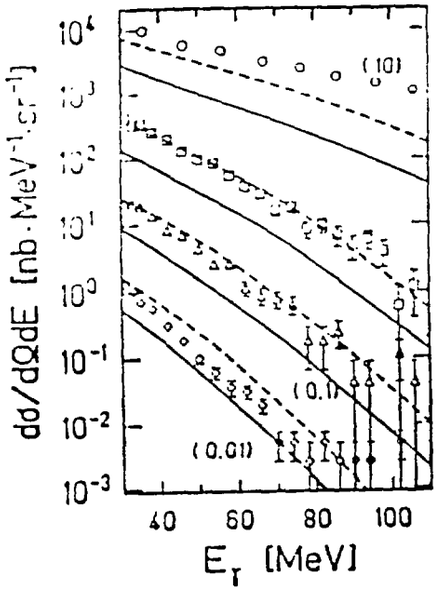

FIGURE 18